

Graphene Covalently Binding Aryl Groups: Conductivity Increases Rather than Decreases

Ping Huang, Huarui Zhu, Long Jing, Yuliang Zhao, and Xueyun Gao*

CAS Key Laboratory for Biomedical Effect of Nanomaterials and Nanosafety, Institute of High Energy Physics, Chinese Academy of Sciences, Beijing 100049, P. R. China

Graphene has been attracting more and more attentions since its discovery in 2004.^{1,2} Its unusual electronic properties, including high carrier mobility and ballistic transport, make graphene to be one of the most promising candidates for the next generation building block of the electronic industry.^{3–8} While its carrier mobility can be as high as $200\,000\text{ cm}^2/(\text{V s})$ ^{9,10} and ballistic transport features can be observed in suspended graphene,¹¹ tuning graphene's electronic property *via* chemical functionalization is still essential to meet different applications.¹²

Absorption of gas molecules,¹³ metal atoms¹⁴ and noble gas atoms¹⁵ on the surface can slightly tune graphene's electronic property, but such approaches are neither controllable nor stable.^{13,15} Covalent chemistry strategy is a more promising way for this purpose. Exposure to H and F plasma can result in hydrogenation¹⁶ and fluorination¹⁷ of graphene, respectively, and an energy gap was opened by these approaches.

Diazonium salts are widely used to functionalize carbon nanotubes¹⁸ and graphene^{19–22} *via* covalent bonds. Since the nitrophenyl group is a typical electron-withdrawing group, previous studies all revealed that covalent bonding of nitrophenyl diazonium salt-functionalized graphene results in a decrease of conductivity.^{19,20} In this work, we show, for the first time, that the conductivity of graphene with nitrophenyl groups covalently bonding to its basal plane can be significantly enhanced when compared to that of the pristine graphene.

RESULTS AND DISCUSSION

Micromechanical exfoliated graphene samples were functionalized by nitrophenyl diazonium salt (4-nitrophenyl diazonium, 4-NPD) tetrafluoroborate as illustrated in Scheme 1. Micro Raman spectroscopy (section S1) and

ABSTRACT Graphene functionalized *via* nitrophenyl groups covalently bonding to its basal plane is studied by Raman spectroscopy and electric transport measurements. The Raman spectra of functionalized graphene exhibit D mode and peaks derived from nitrophenyl groups, and the two fingerprints exhibit nearly the same distribution in the two-dimensional Raman maps over the whole graphene sheet. This result directly proves that the nitrophenyl groups bond to the graphene basal plane *via* σ -bonds. Electric transport measurements demonstrate that the modified graphene is significantly more conductive than intrinsic graphene. In the competition between charge transfer effect and scattering effect introduced by the nitrophenyl groups, the former one is dominant so that the conductivity of functionalized graphene is significantly enhanced as a result.

KEYWORDS: graphene · nitrophenyl groups · Raman spectrum · covalently bonding · conductivity

electronic transport (section S2) measurements were used to investigate our pristine and functionalized graphene samples.

Figure 1 shows the Raman spectra of graphene before and after the chemical modification (see Figure 2a for the optical image of the graphene sample). There are two features in the Raman spectra of pristine graphene, the G mode at $\sim 1585\text{ cm}^{-1}$ and the 2D mode at $\sim 2700\text{ cm}^{-1}$. The single 2D peak and the high ratio of I_{2D}/I_G (which is ~ 6) indicate the high quality of our single-layer graphene samples.²³

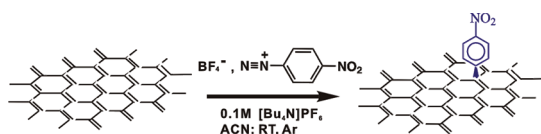
The G mode's position and shape did not change after the chemical modification, implying the reserve of the backbone of the graphene lattice. Otherwise, the G mode will split into two distinct peaks because the 2-fold degeneracy of the TO and LO phonons is lifted by symmetry breaking, as found in carbon nanotubes²⁴ and the aromatic molecule decorated graphene monolayer.²⁵ But one must have noticed that in the Raman spectra of modified graphene, the most significant change is the appearance of the D mode at $\sim 1350\text{ cm}^{-1}$. The D mode is arising from the defect-involved double resonant Raman process at the K point in the Brillouin zone.²⁶ Since the

* Address correspondence to gaoxy@ihep.ac.cn.

Received for review June 23, 2011 and accepted September 18, 2011.

Published online September 19, 2011
10.1021/nn2023232

© 2011 American Chemical Society



Scheme 1. The reaction between graphene and nitrophenyl diazonium salts.

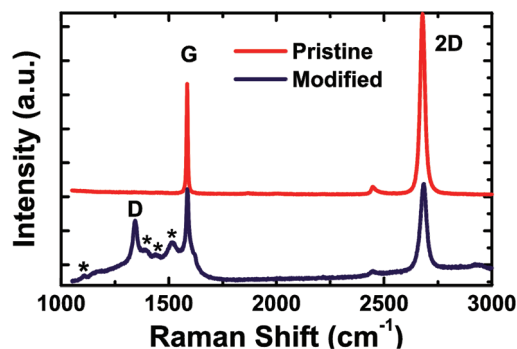


Figure 1. The Raman spectra of pristine and modified graphene. Peaks introduced by nitrophenyl groups are asterisked (*).

backbone of graphene is preserved, we attribute the presence of the D mode to the transition from sp^2 to sp^3 hybridization of the graphene carbon atoms. In fact, the presence of the D mode is generally used to monitor the covalent bonds formed in graphene and widely accepted.^{16,21,27–29} Furthermore, there are some new peaks in the Raman spectrum of modified graphene, at 1108 (C–N symmetric stretching), 1389, 1438, and 1515 cm^{-1} (N–O antisymmetric stretching), respectively. These peaks are derived from the nitrophenyl groups linked to the graphene basal plane as they match the nitrobenzene's Raman spectrum.³⁰ These spectroscopic features shown herein fully demonstrate that we successfully modified graphene *via* chemical reaction, and the result of the corresponding reaction should be the aryl groups connect to the graphene sheets *via* σ -bonds.

Besides the Raman spectra from representative points, more detailed 2-dimensional (2-D) mapping of Raman characteristics of pristine and modified graphene are shown in Figure 2. From the maps of the integrated G mode intensity (Figure 2b, integrated from 1550 to 1610 cm^{-1}), two main domains with sharply distinct G mode intensity can be observed, which exhibits nearly the same patterns as found in the optical images (Figure 2a), that is, the single layer domain on the right exhibits lower G mode intensity while the thicker one on the left exhibits higher intensity. Note that the monotonous increase of the integrated intensity of the G mode under the same measurement conditions is a clue to indicate the increase of the numbers of graphene's stack layers.²³ In the 2-D map of the integrated D mode intensity (Figure 2c, integrated from 1290 to 1400 cm^{-1}), the

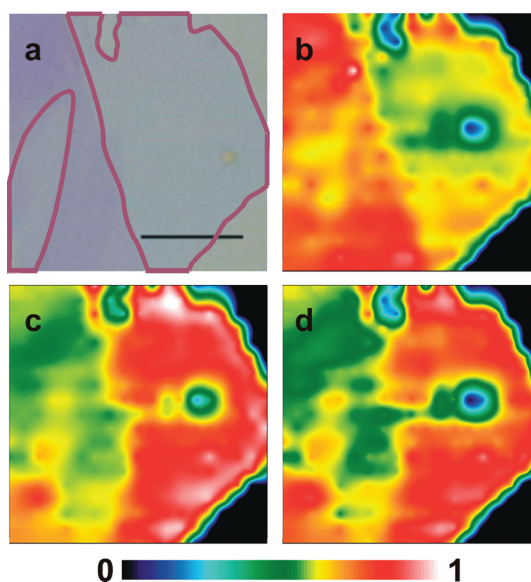


Figure 2. (a) The optical image of the investigated graphene sheet, where the scale bar is 5 μm and single-layer graphene is outlined in the right area. The 2-D Raman maps of (b) the G mode, (c) the D mode, and (d) the N–O vibration mode are shown. The integrated intensity of each Raman mode is normalized. Note that the N–O vibration mode exhibits nearly the same distribution as that of the D mode, which proves that the nitrophenyl groups are bonded with graphene *via* σ -bonds.

intensity distribution is just inverse to that of the G mode. Single layer domains exhibit obviously larger D mode intensity than thicker ones, which are separated by sharp boundaries as shown in the optical image (Figure 2a) and in the G mode map (Figure 2b). The 2-D Raman maps of –NO₂ group (N–O vibration at ~ 1515 cm^{-1} , integrated from 1478 to 1548 cm^{-1} , Figure 2d) shows nearly the same distribution as the D mode in Figure 2c. Since the D mode's intensity maps reflect the distribution of the sp^3 carbon atoms and the intensity map of nitrobenzene's peak indicates the distribution of nitrophenyl groups on graphene sheet, these results prove directly that the appearance of the D mode corresponds to the nitrophenyl groups attaching to graphene *via* σ -bonds, and this functionalization is inhomogeneous over the whole graphene sheet. Our result is consistent with STM study of diazonium salts functionalized epitaxial graphene.²²

To investigate how the modification affects the transport properties of graphene, conventional e-beam lithography was used to fabricate the 4-wire configuration devices, and the devices were measured in a PPMS-9 system (see section S2). Figure 3a shows the temperature dependence of pristine and modified single-layer graphene. It is found that the resistivity of pristine graphene at room temperature is ~ 2350 Ω and exhibits very weak temperature dependence, which is well consistent with previous works.³¹ The functionalization of graphene by nitrophenyl groups causes nearly a 50% decrease of the room temperature resistivity (~ 1350 Ω ; Figure 3a sample 1, reacted with 20 mM 4-NPD for 10 h). While the

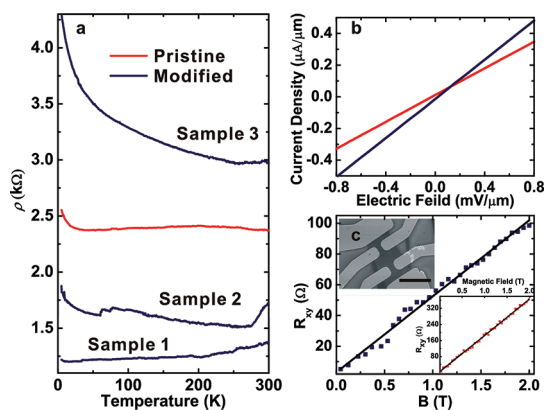


Figure 3. (a) The ρ – T character of pristine graphene and three functionalized graphene samples prepared in different reaction conditions, respectively. (b) I – V character of pristine and modified graphene (sample 1), respectively. (c) Hall effect of modified graphene (sample 1) vs magnetic field. The linear fit of the data is also shown, which gives a hole density of $\sim 1.3 \times 10^{13} \text{ cm}^{-2}$. (Top insert) SEM image of a Hall bar device. Scale bar, 5 μm . (Bottom insert) Hall effect of pristine graphene and linear fit of the data, revealing a hole density of $\sim 3.6 \times 10^{12} \text{ cm}^{-2}$.

temperature dependence is still weak, the resistivity of functionalized graphene decreases monotonically with decreasing temperature. Figure 3b shows the I – V characters of the pristine and modified graphene measured at 300 K. The slope of the curve of the modified graphene is significantly larger than that of the pristine graphene which implies a remarkable increase of conductivity.

To our best knowledge, it is observed for the first time that graphene's room temperature resistivity can be remarkably reduced *via* the chemical groups attaching to the graphene basal plane by sp^3 bonds. However, previous studies showed an increase of the room temperature resistivity when phenyl groups²⁷ and nitrophenyl groups¹⁹ were covalently linked to graphene. We speculate that the difference originates from the extent of the chemical reaction. We find that the reaction extent of these reported samples are less than that of our single-layer samples because the concentration of reagents is higher and the reacting time is longer in our graphene chemical modification processes, which will induce deeper extent of reaction and more nitrophenyl groups will bond to our graphene samples. To prove this, the ρ – T character of another two samples is also shown in Figure 3a labeled as sample 2 (reacted with 15 mM 4-NPD for 10 h) and sample 3 (reacted with 10 mM 4-NPD for 10 h), respectively. The room temperature resistivity of sample 3 ($\sim 3000 \Omega$) is higher than that of pristine graphene and increases monotonically with decreasing temperature below ~ 250 K. Increasing the concentration of reagent solution to 15 mM, however, led to the decrease of resistivity ($\sim 1750 \Omega$). Note that further increasing the concentration of reagent solution to 20 mM led to a further decreasing of resistivity, as shown in sample 1. The intensity of the D mode

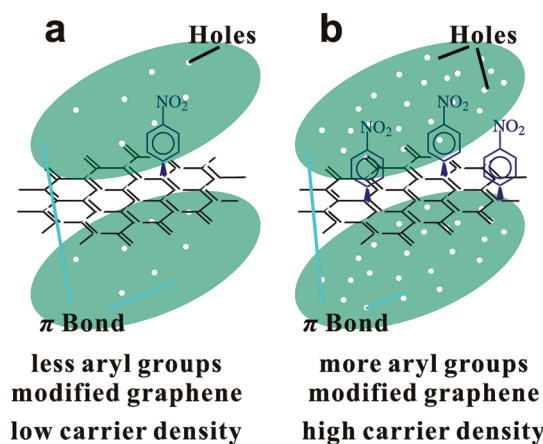


Figure 4. Illustration of charge transfer effect introduced by nitrophenyl groups covalently bonding to graphene basal plane. (a) In the low reaction extent, fewer electrons transfer from the graphene conjugated π -bond to the covalent bonds between graphene and nitrophenyl groups, leaving less holes as charge carriers. In this situation, the scattering effect of nitrophenyl groups is dominant. (b) In high reaction extent, much more holes are formed in the conjugated π -bond and this effect overruns the scattering effect, hence the conductivity is enhanced.

and the $-\text{NO}_2$ compared to those of the the G mode in Raman spectra of those samples give evidence that the coverage of nitrophenyl group on graphene basal plane increases with increasing concentration of reagent solution, the results of which are shown in section S3 in the Supporting Information.

The nitrophenyl groups covalently bonding to graphene mainly introduce two competitive effects: first, electrons will be pulled from graphene's conjugated π -bond into nitrophenyl groups as they are typical electron-withdrawing groups, leaving holes on the graphene basal plane as charge carriers. As more nitrophenyl groups bond to graphene, the carrier density will increase.¹⁹ Second, covalent bonds between graphene and nitrophenyl groups perform as defects so that the scattering probability of the carriers increases, decreasing the mean free path of the carriers, hence lowering their mobility.^{15,32} An energy gap may also open in the band structure and decrease the carrier mobility.²⁸ Note that the conductivity σ can be described as following:

$$\sigma = \mu ne \quad (1)$$

where μ is the carrier mobility, n is carrier density, and e is elementary charge. The evolution with the reaction extent of the two effects introduced by the chemical functionalization of graphene can be described as the following. If the reaction extent is relatively low as reported in the previous works, the nitrophenyl groups linking to the graphene are thus relatively few. In this case, the scattering effect is more obvious than the charge transfer effect, leading to a decrease of the conductivity. However, if the reaction extent exceeds a certain level, the effect of increasing carrier density will

overrun the effect of reducing carrier mobility, resulting in an increase of conductivity. Figure 4 illustrates our understanding of how chemical modification affects graphene's conductivity by charge transfer effect.

To prove this explanation, we further took Hall effect measurement (Figure 3c) on the modified sample; the results gave a very high hole density of $n_p \approx 1.3 \times 10^{13} \text{ cm}^{-2}$ (corresponding to a shift of charge neutrality point to +180 V gate voltage on a 300 nm SiO₂ back gate¹). Note that such a high carrier density cannot originate from the absorption of gas molecules in ambient condition, which shifts the charge neutrality point to ~60 V at the most.^{1,33} In fact, we measured a pristine graphene's carrier density, as shown in Figure 3c inset, which reveals a hole density of $\sim 3.6 \times 10^{12} \text{ cm}^{-2}$. Also the previous reported doping effect by nitrophenyl groups absorbed on graphene leads to the charge neutrality point shifting ~60 V to the positive gate voltage side.³⁴ The hole mobility is calculated to be $\mu_p \approx 370 \text{ cm}^2/(\text{V s})$. This result proves that for

modified graphene with high reaction extent, both charge transfer effect and scattering effect happen, and the former one is more significant than the latter.

But what will happen if much more carbon atoms were transformed from sp² to sp³ hybridization as realized by Elias *et al.*?¹⁶ In this situation, the conjugated π -bonds over the graphene sheet are totally broken down, leading to localization of charge carriers, thus the insulator behavior comes out.

In summary, nitrophenyl groups are successfully attached to graphene *via* covalent carbon–carbon bonds. We further demonstrated that this modification significantly enhances the conductivity of graphene. Since the conductivity of graphene is suppressed in low-reacting ranges, our approach provides an alternate way to increase the conductivity of graphene. Thus, the method of covalently attaching aryl groups to a graphene basal plane can tune the conductivity of graphene either to a higher or lower level depending on the amount of aryl groups bonding on graphene.

EXPERIMENTAL SECTION

Diazonium Functionalization of Graphene. Single-layer graphene was prepared by micromechanical exfoliation of HOPG (Broad Tech System, Inc.) and transferred onto silicon substrates with 300 nm thermally grown oxide.¹ The graphene flakes were first identified by their contrast under an optical microscope and further confirmed by Raman spectroscopy and AFM studies.

The chips were then immersed into 5 mL of fresh degassed (by Ar) acetonitrile (ACN) solution of 10–20 mM 4-nitrophenyl diazonium (4-NPD) tetrafluoroborate and 0.1 M tetrabutylammonium hexafluorophosphate ([Bu₄N]PF₆), which was prepared by dissolving [Bu₄N]PF₆ (0.1937 g, Aldrich, 98%) and 4-NPD (0.01184 g, 0.01777 and 0.02369 g for 10, 15, and 20 mM, respectively) in ACN (5 mL, Beijing chemical works, 99.9%). The chemical reaction between graphene and 4-NPD was carried out at room temperature in Ar atmosphere for 10 h in the absence of light in a glovebox. After the chemical reaction, the samples were washed with ACN flow and then immersed in ACN overnight to remove the residual reagents. Finally, the samples were washed with acetone and blown dried by N₂.

Acknowledgment. This work was supported by 973 Program (2007CB935604, 2009CB930204, 2011CB933400), NSFC (30870677, 31070891), and CAS Knowledge Innovation Program.

Supporting Information Available: Raman spectroscopy, fabrication of the graphene devices and their electric transport measurements and evolution of nitrophenyl groups' coverage on graphene with increasing 4-NPD concentration estimated by Raman spectrum. This material is available free of charge *via* the Internet at <http://pubs.acs.org>.

REFERENCES AND NOTES

- Novoselov, K. S.; Geim, A. K.; Morozov, S. V.; Jiang, D.; Zhang, Y.; Dubonos, S. V.; Grigorieva, I. V.; Firsov, A. A. Electric Field Effect in Atomically Thin Carbon Films. *Science* **2004**, *306*, 666–669.
- Geim, A. K.; Novoselov, K. S. The Rise of Graphene. *Nat. Mater.* **2007**, *6*, 183–191.
- Young, A. F.; Kim, P. Quantum Interference and Klein Tunneling in Graphene Heterojunctions. *Nat. Phys.* **2009**, *5*, 222–226.

- Miao, F.; Wijeratne, S.; Zhang, Y.; Coskun, U. C.; Bao, W.; Lau, C. N. Phase-Coherent Transport in Graphene Quantum Billiards. *Science* **2007**, *317*, 1530–1533.
- Stankovich, S.; Dikin, D. A.; Dommett, G. H.; Kohlhaas, K. M.; Zimney, E. J.; Stach, E. A.; Piner, R. D.; Nguyen, S. B.; Ruoff, R. S. Graphene-Based Composite Materials. *Nature* **2006**, *442*, 282–286.
- Tombros, N.; Jozsa, C.; Popinciuc, M.; Jonkman, H. T.; van Wees, B. J. Electronic Spin Transport and Spin Precession in Single Graphene Layers at Room Temperature. *Nature* **2007**, *448*, 571–574.
- Lin, Y.; Jenkins, K. A.; Valdes-Garcia, A.; Small, J. P.; Farmer, D. B.; Avouris, P. Operation of Graphene Transistors at Gigahertz Frequencies. *Nano Lett.* **2009**, *9*, 422–426.
- Williams, J. R.; DiCarlo, L.; Marcus, C. M. Quantum Hall Effect in a Gate-Controlled P–N Junction of Graphene. *Science* **2007**, *317*, 638–641.
- Bolotin, K. I.; Sikes, K. J.; Jiang, Z.; Klima, M.; Fudenberg, G.; Hone, J.; Kim, P.; Stormer, H. L. Ultrahigh Electron Mobility in Suspended Graphene. *Solid State Commun.* **2008**, *146*, 351–355.
- Morozov, S. V.; Novoselov, K. S.; Katsnelson, M. I.; Schedin, F.; Elias, D. C.; Jaszczak, J. A.; Geim, A. K. Giant Intrinsic Carrier Mobilities in Graphene and Its Bilayer. *Phys. Rev. Lett.* **2008**, *100*, 016602.
- Du, X.; Skachko, I.; Barker, A.; Andrei, E. Y. Approaching Ballistic Transport in Suspended Graphene. *Nat. Nanotechnol.* **2008**, *3*, 491–495.
- Avouris, P. Graphene: Electronic and Photonic Properties and Devices. *Nano Lett.* **2010**, *10*, 4285–4294.
- Schedin, F.; Geim, A. K.; Morozov, S. V.; Hill, E. W.; Blake, P.; Katsnelson, M. I.; Novoselov, K. S. Detection of Individual Gas Molecules Adsorbed on Graphene. *Nat. Mater.* **2007**, *6*, 652–655.
- Kim, K. K.; Reina, A.; Shi, Y.; Park, H.; Li, L.; Lee, Y. H.; Kong, J. Enhancing the Conductivity of Transparent Graphene Films *via* Doping. *Nanotechnology* **2010**, *21*, 285205.
- Chen, J.; Cullen, W. G.; Jang, C.; Fuhrer, M. S.; Williams, E. D. Defect Scattering in Graphene. *Phys. Rev. Lett.* **2009**, *102*, 236805.
- Elias, D. C.; Nair, R. R.; Mohiuddin, T. M.; Morozov, S. V.; Blake, P.; Halsall, M. P.; Ferrari, A. C.; Boukhalov, D. W.; Katsnelson, M. I.; Geim, A. K.; *et al.* Control of Graphene's

- Properties by Reversible Hydrogenation: Evidence for Graphane. *Science* **2009**, 323, 610–613.
17. Robinson, J. T.; Burgess, J. S.; Junkermeier, C. E.; Badescu, S. C.; Reinecke, T. L.; Perkins, F. K.; Zalalutdniov, M. K.; Baldwin, J. W.; Culbertson, J. C.; Sheehan, P. E.; *et al.* Properties of Fluorinated Graphene Films. *Nano Lett.* **2010**, 10, 3001–3005.
 18. Bahr, J. L.; Yang, J.; Kosynkin, D. V.; Bronikowski, M. J.; Smalley, R. E.; Tour, J. M. Functionalization of Carbon Nanotubes by Electrochemical Reduction of Aryl Diazonium Salts: a Bucky Paper Electrode. *J. Am. Chem. Soc.* **2001**, 123, 6536–6542.
 19. Bekyarova, E.; Itkis, M. E.; Ramesh, P.; Berger, C.; Sprinkle, M.; de Heer, W. A.; Haddon, R. C. Chemical Modification of Epitaxial Graphene: Spontaneous Grafting of Aryl Groups. *J. Am. Chem. Soc.* **2009**, 131, 1336–1337.
 20. Sinitskii, A.; Dimiev, A.; Corley, D. A.; Fursina, A. A.; Kosynkin, D. V.; Tour, J. M. Kinetics of Diazonium Functionalization of Chemically Converted Graphene Nanoribbons. *ACS Nano* **2010**, 4, 1949–1954.
 21. Sharma, R.; Baik, J. H.; Perera, C. J.; Strano, M. S. Anomalous Large Reactivity of Single Graphene Layers and Edges Toward Electron Transfer Chemistries. *Nano Lett.* **2010**, 10, 398–405.
 22. Hossain, M. Z.; Walsh, M. A.; Hersam, M. C. Scanning Tunneling Microscopy, Spectroscopy, and Nanolithography of Epitaxial Graphene Chemically Modified with Aryl Moieties. *J. Am. Chem. Soc.* **2010**, 132, 15399–15403.
 23. Graf, D.; Molitor, F.; Ensslin, K.; Stampfer, C.; Jungen, A.; Hierold, C.; Wirtz, L. Spatially Resolved Raman Spectroscopy of Single- and Few-Layer Graphene. *Nano Lett.* **2007**, 7, 238–242.
 24. Pimenta, M. A.; Marucci, A.; Brown, S.; Matthews, M. J.; Rao, A. M.; Eklund, P. C.; Smalley, R. E.; Dresselhaus, G.; Dresselhaus, M. S. Resonant Raman Effect in Single-Wall Carbon Nanotubes. *J. Mater. Res.* **1998**, 13, 2396–2404.
 25. Dong, X.; Shi, Y.; Zhao, Y.; Chen, D.; Ye, J.; Yao, Y.; Gao, F.; Ni, Z.; Yu, T.; Shen, Z.; *et al.* Symmetry Breaking of Graphene Monolayers by Molecular Decoration. *Phys. Rev. Lett.* **2009**, 102, 135501.
 26. Reich, S.; Thomsen, C. Raman Spectroscopy of Graphite. *Philos. Trans. R. Soc.* **2004**, 362, 2271–2288.
 27. Liu, H.; Ryu, S.; Chen, Z.; Steigerwald, M. L.; Nuckolls, C.; Brus, L. E. Photochemical Reactivity of Graphene. *J. Am. Chem. Soc.* **2009**, 131, 17099–17101.
 28. Niyogi, S.; Bekyarova, E.; Itkis, M. E.; Zhang, H.; Shepperd, K.; Hicks, J.; Sprinkle, M.; Berger, C.; Lau, C. N.; DeHeer, W. A.; *et al.* Spectroscopy of Covalently Functionalized Graphene. *Nano Lett.* **2010**, 10, 4061–4066.
 29. Kudin, K. N.; Ozbas, B.; Schniepp, H. C.; Prud, R. K.; Aksay, I. A.; Car, R. Raman Spectra of Graphite Oxide and Functionalized Graphene Sheets. *Nano Lett.* **2008**, 8, 36–41.
 30. El'Kin, P.; Pulin, V.; Kosterina, E. Structural Dynamic Models and Vibrational Spectra of Nitrobenzene and Nitropyridines. *J. Appl. Spectrosc.* **2005**, 72, 483–487.
 31. Skakalova, V.; Kaiser, A. B.; Yoo, J. S.; Obergfell, D.; Roth, S. Correlation Between Resistance Fluctuations and Temperature Dependence of Conductivity in Graphene. *Phys. Rev. B* **2009**, 80, 153404.
 32. Adam, S.; Hwang, E. H.; Galitski, V. M.; Das Sarma, S.; Self-Consistent, A Theory for Graphene Transport. *Proc. Natl. Acad. Sci. U.S.A.* **2007**, 104, 18392–18397.
 33. Yung-Fu, C. E. A. Magnetoresistance in Single-Layer Graphene: Weak Localization and Universal Conductance Fluctuation Studies. *J. Phys.: Condens. Matter* **2010**, 22, 205301.
 34. Farmer, D. B.; Golizadeh-Mojarad, R.; Perebeinos, V.; Lin, Y. M.; Tulevski, G. S.; Tsang, J. C.; Avouris, P. Chemical Doping and Electron-Hole Conduction Asymmetry in Graphene Devices. *Nano Lett.* **2009**, 9, 388–392.